Trajectories of cloud droplets around a rain drop observed in the Mainz vertical wind tunnel

J. Fugal[1,2]*, A. Gorska[1,3], S. K. Mitra[2], S. P. Malinowski[2,3], Miklos Szakall[2], Nadine von Blohn[2], Alexander Jost[1], Stephan Borrmann[1,2]

[1] Max Planck Institute for Chemistry, Mainz, Germany
[2] Institute of Atmospheric Physics, Johannes Gutenberg University, Mainz, Germany
[3] Institute of Geophysics, Faculty of Physics, University of Warsaw, Warsaw, Poland

1. INTRODUCTION

Measurements of rain drop and cloud droplet collision efficiency were first made a half a century ago, i.e. (Kinzer and Cobb, 1958; Beard and Pruppacher, 1971). These first laboratory measurements are summarized in Abbott (1977). These experiments were done by observing growth rates then calculating collision efficiencies. For example, experiments were made by placing a drop in known droplet and relative velocity conditions, measuring the drop mass at the start and end of droplet collection, and then inferring the collision efficiency. This procedure directly measures the collection integral and infers the integrand while making the assumption that the measured droplet, flow, and evaporation conditions are constant. An example of such measurements include Vohl et al. (1999) and Vohl et al. (2007).

With the coming of digital holographic particle tracking velocimetry (DHPTV), we can now directly measure the integrand of the collection integral by making time–resolved measurements of collisions. Presented here is proof of concept of such measurements using digital holography in the Mainz vertical wind tunnel to examine drop–droplet collisions in a laminar flow.

There are at least four advantages of DHPTV over the traditional method of measuring collision efficiency, including (1) time–resolved collisions and near—collisions. Although our measurements are low resolution, higher resolution measurements would reveal actual drop–droplet interaction on the collision scale. The second (2) advantage is one also sees the timing of the collisions in which one can examine the stochastic nature of collection. Another advantage (3), because the droplets seeded into the flow have low Stokes number, they also simultaneously reveal the flow velocity field, i.e. that the flow is laminar. Finally, a further advantage (4) of this tracking is that since the droplets are size–resolved, even with a broad droplet size distribution, one can simultaneously measure the collision efficiency for each drop and droplet size.

One disadvantage of this process is that current DHPTV technology can record less than a minute of collisions and sometimes just a few seconds, where the traditional method allows the drop to collect droplets for tens of minutes (Vohl et al., 1999).

2. METHOD AND EXPERIMENTAL SETUP

To make DHPTV measurements of drop–droplet collisions, a laser and camera were placed as shown in Fig. 1 about the measurement section of the wind tunnel.

The section has a 17×17 cm^2 cross section. A 600–700 μm droplet is injected via a syringe and tube into the section which is then brought down and floated at the sample volume level by adjusting the vertical velocity of the tunnel to the terminal velocity of the drop. The flow organization in the Mainz vertical wind tunnel is presented in Fig. 2.

*Corresponding author's address: Hahn-Meitner-Weg 1, 55128 Mainz; E-Mail: jacob.fugal@mpic.de

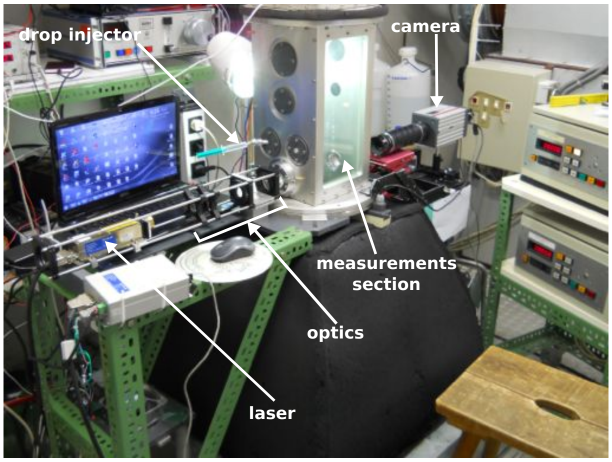

Figure 1: Measurement section of the Mainz vertical wind tunnel with mounted holography setup: the laser, optics and the camera. Drops are injected just above the measurement volume with the drop injector.

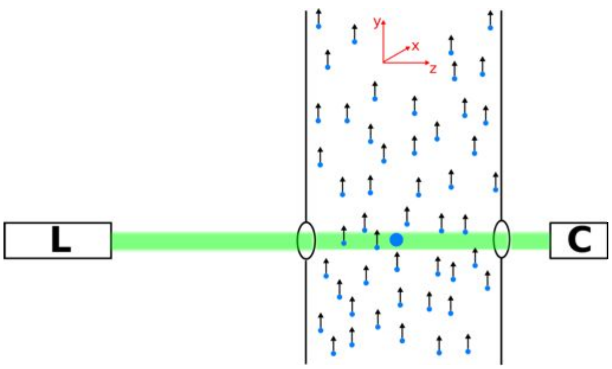

Figure 2: Flow configuration in the Mainz vertical wind tunnel with marked measurement volume (L – laser, C – camera).

The terminal velocity for this size of droplet is about 2.9 m/s. The laminar flow is seeded with droplets of size 10–70 μm as shown in the size distribution in Fig. 3.

The laser (CryLas FTSS355-Q3 with the 532 nm option) is a pulsed Nd:YAG, frequency doubled to 532 nm, with a passive Q switch which makes 1 ns pulses and is fired at 1040 Hz matching the cameras frame rate. The camera (MotionPro X3) has a 1280×1024, 12 μm pixel CMOS sensor that runs at 1040 fps saving to 8 GB of onboard RAM that allows about 5 seconds of recording before one must stop to download the images. We placed the longer axis (1280 pixels) vertically so we could record longer tracks about the drop. We used a 100 mm f/4 lens with extension rings which gave us a 9.15 μm effective pixel size. The sample volume in the section is then 9.4 × 11.7 × 170 mm^3. With a 11.7 mm vertical length and almost 3 m/s, we are able to obtain 4 or 5 point tracks for the droplets as they pass through the sample volume.

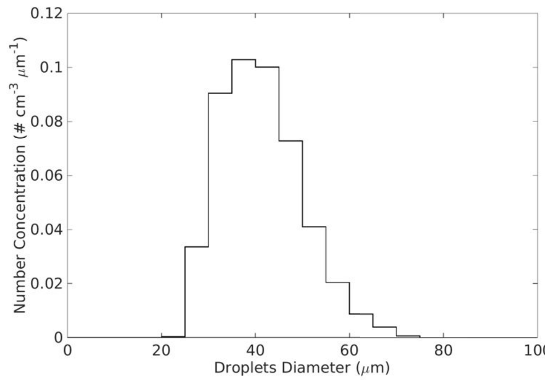

Figure 3: Droplet size distribution.

The most difficult part of the measurement is injecting the drop such that is falls and is floated in the holographic sample volume. With effort and a bit of luck one can get the drop in the section for 1 second, and then hit the camera post-trigger to stop the camera and download the 1 second of holograms to the computer. With a great deal of effort and even more luck, we were able to obtain 5 continuous seconds of holograms with the drop in the frame. Naturally, it is this 5 seconds used to show collisions in this work.

In order to achieve proof of concept, we used the simplest and easiest possible conditions to measure these collisions. This includes our choice of drop and droplet size and vertical velocity. The 700 μm drop is large enough that one can see it to keep it floating in the sample volume. The 40 μm average size droplets are easily resolvable in the holograms. And 4 to 5 point tracks are all that are required to document collisions although it is insufficient to really resolve the droplet trajectories of those that narrowly miss the drop. After we have established proof of concept, we intend to expand to conditions of more interest in clouds such as smaller drops and droplets.

3. HOLOGRAM ANALYSIS FOR TRACKING THE DROP

To search for drop-droplet collisions, we need to track both drop and droplets. To track the drop, we used HOLOSUITE (Fugal et al., 2009) to first

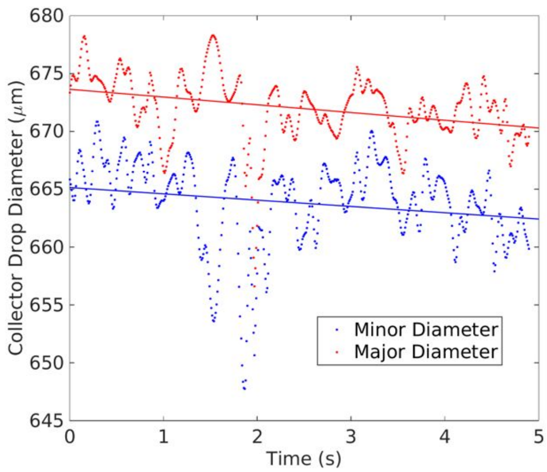

Figure 4: Time dependence of drop diameter. Because of drop asphericity, plotted are two parameters: minor and major diameter. The plot shows that the drop size decreases. That means that evaporation of the drop is stronger than its growing by collision–coalescence.

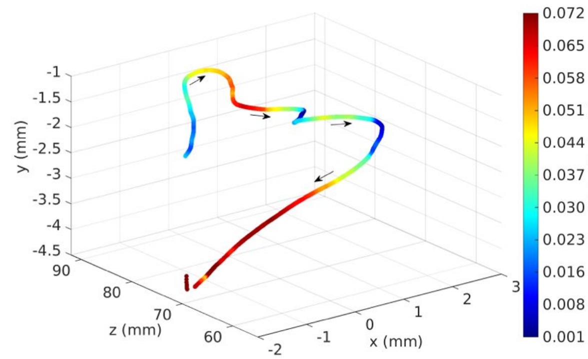

Figure 5: Drop trajectory in the measurement volume (orientation in agreement with Fig. 1 and Fig. 2). Direction of the drop movement (rising hologram numbers, time flow) is marked with black arrows. Color depicts drop speed.

apply filtering to the holograms appropriate to make the background field flatter and remove most of the noise without altering the drop's appearance in each hologram. Because there is only one drop per hologram, we then used a solving routine in HOLOSUITE to find the drop's location in each hologram and then calculate the statistics of the drop's in-focus position. Tracking the drop is trivial as it appears in each hologram only once. From that we examined the drop's size (Fig. 4) and velocity in time (Fig. 5).

The drop's shape shows weak asphericity (compare minor and major diameters in Fig. 4) perhaps due to its fall (Szakall et al., 2010). Jones and Saylor (2009) shows that for drops of diameters of 1.36 mm axis ratio is of about 5 %, so for drops half that size it should be far less than 5 %. Roughly calculated axis ratio for our drop is about 1–2 %. The drop's size plot (Fig. 4) shows that its size shrinks in time, about 10 μm (1 pixel) in 5 seconds. In this case, evaporation is apparently stronger than growth by collision–coalescence.

Fig. 5 shows the drop trajectory in the measurement volume. Black arrows show the direction of the drop motion. The color axis depicts the drop velocity which is calculated based on drop positions obtained from holograms reconstruction and known time interval between consecutive holograms. The drop positions were first filtered due to the rather large noise in the dimension along the optical axis, often called the z-axis or z-position of the drop. The drop speed in this hologram series varies over almost 2 orders of magnitude due to evaporation and the slightly irregular velocity field in the wind tunnel and the constant manual adjustment of the wind-tunnel vertical velocity.

4. HOLOGRAM ANALYSIS FOR TRACKING THE DROPLETS

The droplets are more difficult to track, but still rather simple because the droplet concentration was so low (about 2 cm^{-3}), which makes about 40 or 50 per hologram. The droplets were small enough, that sometimes the signal of a particular droplet is too low to be automatically detected in one hologram, and so a calculated track ends early even though the droplet was still there. To track the droplets, we used HOLOSUITE filters that remove everything larger than the maximum drop size without losing or distorting the droplet signal. After reconstruction, we connected droplets from one hologram to the next using the known mean velocity of the flow and looking for the nearest neighbor to the predicted location of where one drop should appear in the next hologram. This worked most of the time for the droplets, but as mentioned before, there are still tracks that are missing droplets, that end early, and contain other errors. However, the accuracy is high enough to examine the flow velocity field and to look for collisions for proof of concept.

Having the droplet positions, we were able to calculate droplet velocities. Fig. 6 shows droplet

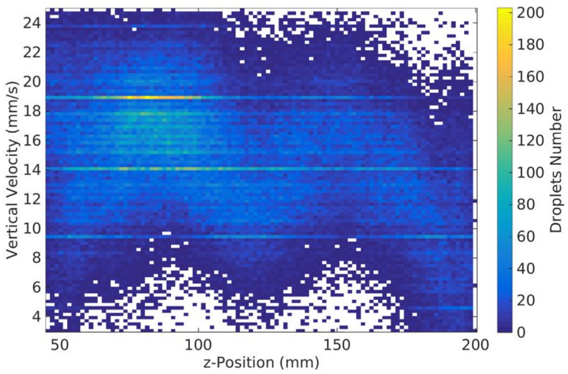

Figure 6: Lateral velocity dependence on their z position shows a non-uniform flow field in this cross–section. The lower lateral velocities are observed in the center of the wind tunnel and close to both sides of the measurement section (z = 50 mm is on the camera side and z = 200 mm is on the laser side). On the camera side seems to be more droplets detected.

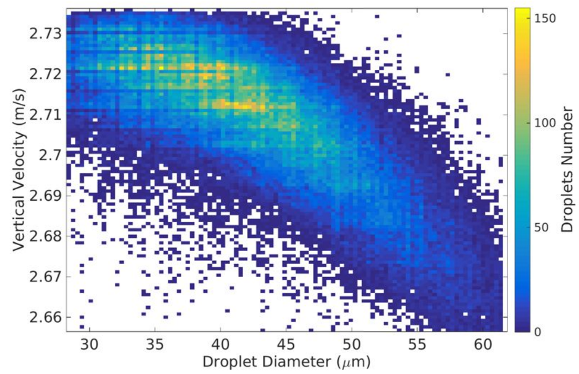

Figure 7: Droplets vertical velocity dependence on their diameters shows terminal velocity dispersion for the droplet diameter range.

lateral velocity dependence on z-position and the flow velocity profile in this dimension. Lower velocities are observed in the center of the wind tunnel and close to both sides of the measurement section. On the camera side seems to be more droplets detected. Also the drops seemed to prefer to the camera side. We could not measure such a structure in the second horizontal direction as it has only 8 mm range and does not cover whole measurement section width.

Further analysis showed that droplet size and vertical velocity were unbiased by or uniform with droplet position in the sample volume. However droplet size had a strong correlation with its vertical velocity (Fig. 7) showing the expected dependence of terminal velocity on droplet size.

5. TRACKING THE DROPLETS IN THE FRAME OF THE DROP AND SEARCHING FOR COLLISIONS

To scan for collisions, we searched for droplet tracks that passed the drop within a fraction of the collector drop diameter. We then searched manually through these tracks to see if the droplets collided with the drop or not. We have only 4 or 5 point tracks, with considerable noise in the z-direction. Our only reliable way of knowing if there was a collision is if the droplet did not continue after approaching the big drop. As the tracking code is not accurate in every case, we checked the hologram reconstructions by hand to confirm that a droplet approached but did not pass the drop. We have confirmed 8 collisions and show 2 examples in Fig. 8 and Fig. 9. The first one (Fig. 8) is almost centred and was observed at the beginning of the set.

The second one (Fig. 9) is not centered. In the x and y plot (lower panel), the droplet looks like it hits the edge of the drop and raises the question whether it still was a collision. That is why manual confirmation was needed and allowed us to keep this case. The droplet was visible on three holograms below the drop and was not visible in the next two holograms.

Tab. 1 includes a list of the collisions we found complete with the droplets sizes. It is interesting that we have 4 collisions at the very beginning of the third second of the measurement time and no collisions until the fifth second. They are not uniformly distributed in time. This might be due to detection errors or variation in a stochastic process. Diameters of colliding droplets cover almost the whole range of droplets diameters observed in the flow.

6. CONCLUSIONS AND FUTURE WORK

We proved that with use of in–line holography we can observe trajectories of collisions and near–collisions of cloud droplets with rain drops in the Mainz vertical wind tunnel. We found and confirmed 8 collisions so far in 5.5 seconds of data. Beside drop and droplet positions and velocities, we can also obtain their sizes and are able to characterize the flow (velocity field).

We still have about 45 s of the same data set to analyze which represents a chance to find about 75 collisions more. We will automate detection

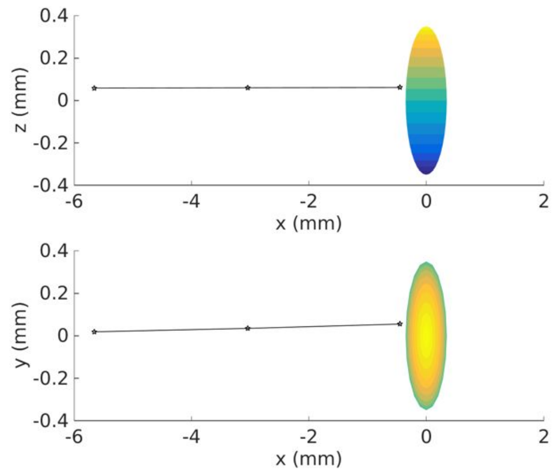

Figure 8: First observed collision, almost centered, in the analyzed hologram series in 621 ms from the beginning of the set. The droplet moves left to right along the x axis. Z is the optical axis.

Table 1: A list of the collisions we found complete with the droplets sizes.

Collision	Time [ms]	Droplet diameter [μm]
1	621	35
2	1084	33
3	2004	40
4	2125	49
5	2229	33
6	2250	39
7	4164	60
8	4304	44

of collisions and near–collisions to make possible the analysis of longer data sets without needing to manually monitor every collision possibility. We plan to automate drop injection which will allow the user to focus only on adjusting the terminal velocity of the drop. We hope to perform more measurements of different droplet and drop sizes with a higher–resolution and higher frame–rate camera to get better resolved tracks.

ACKNOWLEDGEMENTS
We acknowledge the financial support of the Max Planck Institute of Chemistry for Anna Gorska, and the writers of the HOLOSUITE software which was used to process the holograms.

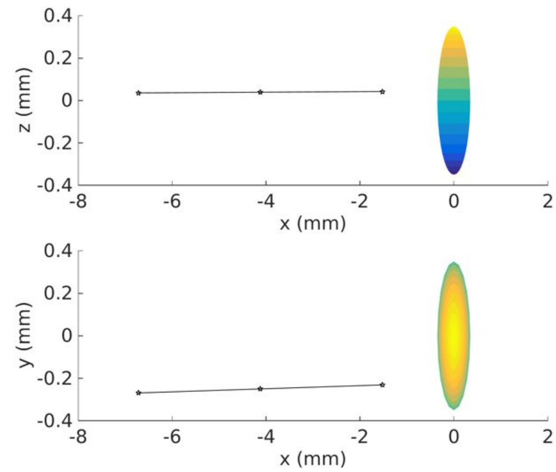

Figure 9: Last observed collision in analysed hologram series in 4304 ms from the beginning of the set. This collision was manually confirmed with reconstructed holograms. The droplet was visible on three holograms below the drop and was not visible in any more of the next few holograms.

References

C. E. Abbott. A Survey of Waterdrop Interaction Experiments. *Rev. Geophys.*, 15(3):363–374, 1977.

K. V. Beard and H. R. Pruppacher. A wind tunnel investigation of collection kernels for small water drops in air. *Q. J. R. Meteorol. Soc.*, 97:242–248, 1971.

J. P. Fugal, T. J. Schulz, and R. A. Shaw. Practical methods for automated reconstruction and characterization of particles in digital in-line holograms. *Measurement Science and Technology*, 20:075501, 2009.

B. K. Jones and J. R. Saylor. Axis Ratios of Water Drops Levitated in a Vertical Wind Tunnel. *J. Atmos. Oceanic Technol.*, 26:2413–2419, 2009. doi:10.1175/2009JTECHA1275.1.

G. D. Kinzer and W. E. Cobb. Laboratory measurements and analysis of the growth and collection efficiency of cloud droplets. *J. Meteor.*, 15: 138–148, 1958.

M. Szakall, S. K. Mitra, K. Diehl, and S. Borrmann. Shapes and oscillations of falling raindrops – A review. *Atmos. Res.*, 97:416–425, 2010.

O. Vohl, S. K. Mitra, S. Wurzler, and H. R. Pruppacher. A Wind Tunnel Study of the Effects of Turbulence on the Growth of Cloud Drops by Collision and Coalescence. *J. Atmos. Sci.*, 56: 4088–4099, 1999.

O. Vohl, S. K. Mitra, S. Wurzler, K. Diehl, and H. R. Pruppacher. Collision efficiencies empirically determined from laboratory investigations of collisional growth of small raindrops in a laminar flow field. *J. Atmos. Res.*, 85:120–125, 2007. doi:10.1016/j.atmosres.2006.12.001.